

# Search for $CP$ Violation in Charged- $\Xi$ and $\Lambda$ Hyperon Decays

T. Holmstrom,<sup>10</sup> N. Leros,<sup>6</sup> R.A. Burnstein,<sup>5</sup> A. Chakravorty,<sup>5</sup> A. Chan,<sup>1</sup> Y.C. Chen,<sup>1</sup> W.S. Choong,<sup>2,7</sup> K. Clark,<sup>9</sup> E.C. Dukes,<sup>10,\*</sup> C. Durandet,<sup>10</sup> J. Felix,<sup>4</sup> Y. Fu,<sup>7</sup> G. Gidal,<sup>7</sup> P. Gu,<sup>7</sup> H.R. Gustafson,<sup>8</sup> C. Ho,<sup>1</sup> M. Huang,<sup>10</sup> C. James,<sup>3</sup> C.M. Jenkins,<sup>9</sup> T. Jones,<sup>7</sup> D.M. Kaplan,<sup>5</sup> L.M. Lederman,<sup>5</sup> M.J. Longo,<sup>8</sup> F. Lopez,<sup>8</sup> L.C. Lu,<sup>10</sup> W. Luebke,<sup>5</sup> K.B. Luk,<sup>2,7</sup> K.S. Nelson,<sup>10</sup> H.K. Park,<sup>8</sup> J.-P. Perroud,<sup>6</sup> D. Rajaram,<sup>5</sup> H.A. Rubin,<sup>5</sup> P.K. Teng,<sup>1</sup> J. Volk,<sup>3</sup> C.G. White,<sup>5</sup> S.L. White,<sup>5</sup> and P. Zyla<sup>7</sup>

(HyperCP Collaboration)

<sup>1</sup>*Institute of Physics, Academia Sinica, Taipei 11529, Taiwan, Republic of China*

<sup>2</sup>*University of California, Berkeley, California 94720, USA*

<sup>3</sup>*Fermi National Accelerator Laboratory, Batavia, Illinois 60510, USA*

<sup>4</sup>*Universidad de Guanajuato, 37000 León, Mexico*

<sup>5</sup>*Illinois Institute of Technology, Chicago, Illinois 60616, USA*

<sup>6</sup>*Université de Lausanne, CH-1015 Lausanne, Switzerland*

<sup>7</sup>*Lawrence Berkeley National Laboratory, Berkeley, California 94720, USA*

<sup>8</sup>*University of Michigan, Ann Arbor, Michigan 48109, USA*

<sup>9</sup>*University of South Alabama, Mobile, Alabama 36688, USA*

<sup>10</sup>*University of Virginia, Charlottesville, Virginia 22904, USA*

(Dated: December 13, 2004)

We have compared the  $p$  and  $\bar{p}$  angular distributions in 117 million  $\Xi^- \rightarrow \Lambda\pi^- \rightarrow p\pi^-\pi^-$  and 41 million  $\bar{\Xi}^+ \rightarrow \bar{\Lambda}\pi^+ \rightarrow \bar{p}\pi^+\pi^+$  decays using a subset of the data from the HyperCP experiment (E871) at Fermilab. We find no evidence of  $CP$  violation, with the direct- $CP$ -violating parameter  $A_{\Xi\Lambda} \equiv (\alpha_{\Xi}\alpha_{\Lambda} - \bar{\alpha}_{\Xi}\bar{\alpha}_{\Lambda})/(\alpha_{\Xi}\alpha_{\Lambda} + \bar{\alpha}_{\Xi}\bar{\alpha}_{\Lambda}) = [0.0 \pm 5.1(\text{stat}) \pm 4.4(\text{syst})] \times 10^{-4}$ .

PACS numbers: 11.30.Er, 13.30.Eg, 14.20.Jn

In the standard model,  $CP$  asymmetries are expected to be ubiquitous in weak interaction processes, albeit often vanishingly small. To date,  $CP$  asymmetries have been seen only in the decays of  $K_L^0$  [1] and  $B_d$  mesons [2]. Although the asymmetries observed in these decays are consistent with standard-model predictions, exotic sources of  $CP$  violation have not been ruled out. Hence it is vital to search for novel sources of  $CP$  violation. Hyperon decays offer promising possibilities for such searches as they are sensitive to sources of  $CP$  violation that, for example, neutral kaon decays are not [3, 4]. The most experimentally accessible  $CP$ -violating signature in spin- $\frac{1}{2}$  hyperon decays is the difference between hyperon and anti-hyperon decay distributions in their parity-violating two-body weak decays. In such decays the angular distribution of the daughter baryon is  $dN/d\Omega = N_0(1 + \alpha\vec{P}_p \cdot \hat{p}_d)/4\pi$ , where  $\vec{P}_p$  is the parent polarization,  $\hat{p}_d$  is the daughter baryon direction, and  $\alpha = 2\text{Re}(S^*P)/(|S|^2 + |P|^2)$ , with  $S$  and  $P$  the  $l = 0$  (parity-odd) and  $l = 1$  (parity-even) final-state amplitudes.  $CP$  invariance requires that  $\alpha = -\bar{\alpha}$  [5].

In HyperCP, the  $\Xi^-$  and  $\bar{\Xi}^+$ 's were produced at an average angle of  $0^\circ$  so that their polarization was zero. The angular distribution of  $p$ 's from unpolarized  $\Xi^-$ 's in  $\Xi^- \rightarrow \Lambda\pi^- \rightarrow p\pi^-\pi^-$  decays is given by

$$\frac{dN}{d\cos\theta} = \frac{N_0}{2}(1 + \alpha_{\Xi}\alpha_{\Lambda}\cos\theta), \quad (1)$$

since the daughter  $\Lambda$  is produced in a helicity state with polarization  $\alpha_{\Xi}$  [6]. The polar angle  $\theta$  is measured in that

$\Lambda$  rest frame, called the lambda helicity frame, in which the direction of the  $\Lambda$  in the  $\Xi^-$  rest frame defines the polar axis. The angular distribution of the  $\bar{p}$  from the corresponding decay sequence,  $\bar{\Xi}^+ \rightarrow \bar{\Lambda}\pi^+ \rightarrow \bar{p}\pi^+\pi^+$ , should be identical *if  $CP$  is not violated*, as both  $\alpha_{\Xi}$  and  $\alpha_{\Lambda}$  reverse sign. Any difference in the angular distributions is evidence of  $CP$  violation in either  $\Xi$  or  $\Lambda$  decays, or perhaps both. The measured  $CP$ -violating observable is

$$A_{\Xi\Lambda} \equiv \frac{\alpha_{\Xi}\alpha_{\Lambda} - \bar{\alpha}_{\Xi}\bar{\alpha}_{\Lambda}}{\alpha_{\Xi}\alpha_{\Lambda} + \bar{\alpha}_{\Xi}\bar{\alpha}_{\Lambda}} \approx A_{\Xi} + A_{\Lambda}, \quad (2)$$

where  $A_{\Xi} \equiv (\alpha_{\Xi} + \bar{\alpha}_{\Xi})/(\alpha_{\Xi} - \bar{\alpha}_{\Xi})$  and  $A_{\Lambda} \equiv (\alpha_{\Lambda} + \bar{\alpha}_{\Lambda})/(\alpha_{\Lambda} - \bar{\alpha}_{\Lambda})$ .

The most recent standard-model calculation for the combined asymmetry is  $-0.5 \times 10^{-4} \leq A_{\Xi\Lambda} \leq 0.5 \times 10^{-4}$  [7]. Note that this prediction uses a theoretical calculation of the  $S$ - and  $P$ -wave  $\Lambda\pi$  final-state scattering phase-shift differences rather than more recent measurements [8]. Non-standard-model calculations, such as left-right symmetric models [9] and supersymmetric models [10, 11], allow for much larger asymmetries. The supersymmetric calculation of He *et al.* [10] generates values of  $A_{\Lambda}$  as large as  $19 \times 10^{-4}$ . Bounds from  $\epsilon$  and  $\epsilon'/\epsilon$  in  $K^0$  decays limit  $A_{\Xi\Lambda}$  to be less than  $97 \times 10^{-4}$  [4]. Experiments have yet to probe hyperon  $CP$  asymmetries beyond the  $O(10^{-2})$  level, with the best limit being  $A_{\Xi\Lambda} = +0.012 \pm 0.014$  [12]. In this Letter we present an experimental search with significantly improved sensitivity.

Data were taken at Fermilab using a high-rate spectrometer (Fig. 1) [13]. The hyperons were produced by an

800 GeV/c proton beam incident at  $0^\circ$  on a  $2 \times 2 \text{ mm}^2$  Cu target. Immediately after the target was a 6.096 m long curved collimator embedded in a dipole magnet (“hyperon magnet”). Charged particles following the central orbit of the collimator exited upward at 19.51 mrad to the incident proton beam direction with a momentum of 157 GeV/c. Following the collimator was a 13 m long evacuated pipe (“vacuum decay region”). The momenta of charged particles were measured using nine multiwire proportional chambers (MWPCs), four in front and five behind two dipole magnets (“analyzing magnets”). At the rear of the spectrometer were two scintillator hodoscopes used in the trigger: one, the same-sign (SS) hodoscope, situated to the beam-left of the charged secondary beam, the other, the opposite-sign (OS) hodoscope, situated to beam-right. A hadronic calorimeter was used to trigger on the energy of the  $p$  or  $\bar{p}$ .

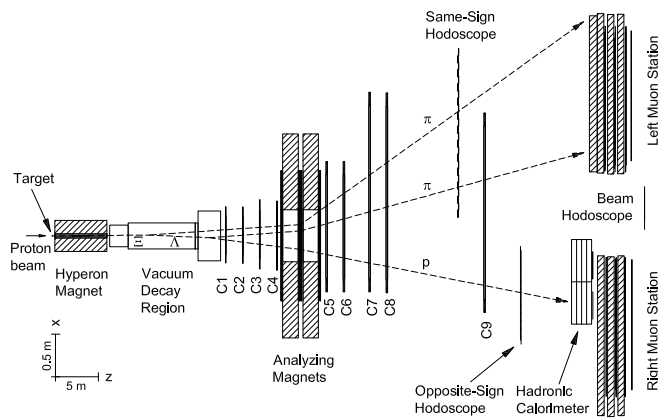


FIG. 1: Plan view of the HyperCP spectrometer.

The  $\Xi^-$  (negative) and  $\Xi^+$  (positive) data were taken alternately, typically with three positive runs followed by one negative run in a sequence that usually took about 12 hours. To switch from one running mode to the other, the polarities of the hyperon and analyzing magnets were reversed and the targets were interchanged; differing target lengths were used to keep the secondary-beam rates approximately equal. At a nominal primary proton beam rate of  $7.5 \times 10^9 \text{ s}^{-1}$  the secondary-beam rate was  $13 \times 10^6 \text{ s}^{-1}$ , with the average difference between the positive and negative rates less than 5%. A simple trigger — the “cascade” (CAS) trigger — with large acceptance and single-bucket (18.9 ns) time resolution was used to select events with the  $\Lambda \rightarrow p\pi^-$  topology. It required the coincidence of at least one hit in each of the SS and OS hodoscopes — the “left-right” (LR) subtrigger — along with at least  $\approx 40$  GeV energy deposited in the hadronic calorimeter, an amount well below that of the lowest energy  $p$  or  $\bar{p}$ .

A total of 90 billion CAS triggers were recorded in the 1999–2000 running period. This analysis used data taken from the end of the run: a 21-day period in December,

1999 and a 12-day period in January, 2000. (The intervening period was devoted to special polarized  $\Xi$  runs.) The dataset included 19% of all the good  $\Xi^+$  events (41.4 million) and 14% of all the good  $\Xi^-$  events (117.3 million) taken in the 1999–2000 running period. The data were divided into 18 analysis sets of roughly equal size, each containing at least three positive and one negative run taken closely spaced in time.

The data were analyzed by a computer program that reconstructed tracks and determined particle momenta, invariant masses, and decay vertices, assuming the  $\Xi \rightarrow \Lambda\pi$  and  $\Lambda \rightarrow p\pi$  hypotheses. Efficiencies of each MWPC wire and hodoscope counter were measured on a run-by-run basis using tracks from reconstructed  $\Xi^\pm$ ,  $K^\pm$ , and  $\Omega^\pm$  events. These efficiencies were typically  $\approx 99\%$  and  $> 99\%$  for the MWPCs and hodoscopes, respectively. The calorimeter trigger efficiency, as determined on a run-by-run basis using good  $\Xi^\pm$  events from the LR trigger, was  $> 99\%$ . Runs with anomalously low ( $\lesssim 95\%$ ) hodoscope, wire chamber, or calorimeter efficiencies were not used; these were less than 5% of the total. The criteria used to select the final event samples were: (1) that the  $p\pi$  and  $p\pi\pi$  invariant masses be, respectively, within  $\pm 5.6 \text{ MeV}/c^2$  ( $3.5\sigma$ ) and  $\pm 3.5 \text{ MeV}/c^2$  ( $3.5\sigma$ ) of the mean values of the  $\Xi$  and  $\Lambda$  masses ( $1.3220$  and  $1.1158 \text{ GeV}/c^2$ ); (2) that the  $z$  coordinate of the  $\Xi$  and  $\Lambda$  decay vertices lie within the vacuum decay region and that the  $\Lambda$  decay vertex precede the  $\Xi$  decay vertex by no more than 0.50 m; (3) that the reconstructed  $\Xi$  trajectory trace back to within  $\pm 2.45 \text{ mm}$  ( $3.3\sigma$ ) and  $\pm 3.26 \text{ mm}$  ( $3.4\sigma$ ), respectively, in  $x$  and  $y$ , of the center of the target; (4) that the  $\Xi$  trajectory trace back to within  $+8.2/-8.4 \text{ mm}$  and  $\pm 6.5 \text{ mm}$ , respectively in  $x$  and  $y$ , from the center of the exit of the collimator; and (5) that the  $\pi^\pm\pi^\pm\pi^\mp$  invariant mass be greater than  $0.5 \text{ GeV}/c^2$  (to remove  $K^\pm \rightarrow \pi^\pm\pi^\pm\pi^\mp$  decays). Cuts on the particle momenta and the numbers of SS and OS hodoscope hits were also made. Events satisfying these criteria had

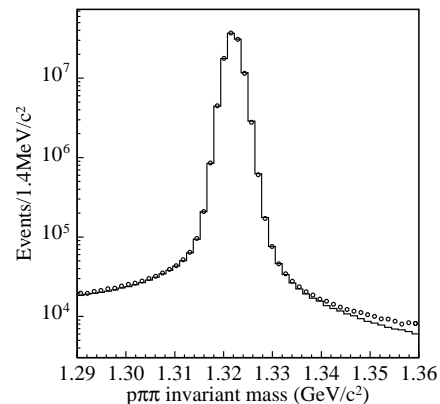


FIG. 2: The unweighted  $p\pi^-\pi^-$  (histogram) and  $\bar{p}\pi^+\pi^+$  (circles) invariant masses.

a background to signal ratio of  $(0.43 \pm 0.03)\%$  for the  $\Xi^-$  data and  $(0.41 \pm 0.03)\%$  for the  $\Xi^+$  data (Fig. 2).

The  $CP$  asymmetry  $A_{\Xi\Lambda}$  was extracted by comparing the  $p$  and  $\bar{p} \cos \theta$  distributions in the lambda helicity frame. As care was taken to exactly reverse the hyperon and analyzing magnetic fields — the fractional difference between the magnitudes of positive and negative analyzing magnet fields was  $\approx 3 \times 10^{-4}$  — biases due to spatial acceptance differences were minimal. The magnetic field magnitudes were updated on a spill-by-spill basis using values recorded by Hall probes placed in each magnet. Differences in the MWPC wire efficiencies were typically on the order of  $1 \times 10^{-3}$  in the secondary beam region, and much less outside. Hodoscope counter efficiency differences were typically much less than  $1 \times 10^{-3}$ . These efficiency differences had negligible effects on  $A_{\Xi\Lambda}$ . The calorimeter efficiency difference was  $\approx 1 \times 10^{-3}$ , and, within errors, uniform over the calorimeter face.

To eliminate differences in the  $\Xi^-$  and  $\Xi^+$  momentum and position distributions, the  $\Xi^-$  and  $\Xi^+$  events were weighted in the three momentum-dependent parameters of the  $\Xi$ 's at the collimator exit (their effective production point): the momentum ( $p_{\Xi}$ ), the  $y$  coordinate ( $y_{\Xi}$ ), and the  $y$  slope ( $s_{\Xi y}$ ). Each parameter was binned in 100 bins for a total of  $10^6$  bins. The  $p_{\Xi}$ ,  $y_{\Xi}$ , and  $s_{\Xi y}$  bin widths were, respectively, 2.25 GeV/ $c$ , 0.13 mm, and  $0.08 \times 10^{-3}$ . Bins with fewer than four events of either polarity had their weights set to zero. After the weights were computed the  $p$  (or  $\bar{p}$ )  $\cos \theta$  of each event was weighted appropriately and the ratio of the weighted  $p$  and  $\bar{p} \cos \theta$  distributions was then formed. The expected ratio,

$$R = C \frac{1 + \alpha_{\Xi\Lambda} \cos \theta}{1 + (\alpha_{\Xi\Lambda} - \delta) \cos \theta}, \quad (3)$$

determined using Eq. (1), was fit to the data to extract the asymmetry  $\delta \equiv \alpha_{\Xi\Lambda} - \bar{\alpha}_{\Xi\Lambda} \cong 2\alpha_{\Xi\Lambda} \cdot A_{\Xi\Lambda}$  and the scale factor  $C$ , where  $\alpha_{\Xi\Lambda} = -0.294$  [14] was used. No acceptance or efficiency corrections were made.

Figure 3 shows typical ratios of weighted and unweighted  $p$  to  $\bar{p} \cos \theta$  distributions from analysis set 1. Figure 4 shows  $\delta$  for all 18 analysis sets. Fits

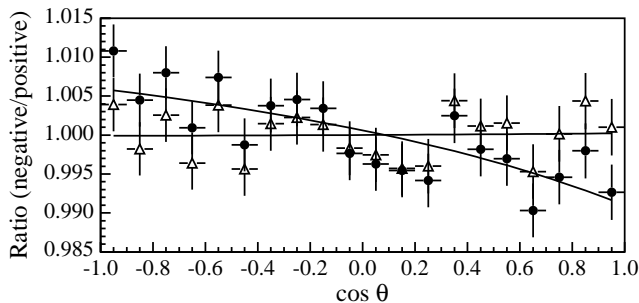


FIG. 3: Ratios of  $p$  to  $\bar{p} \cos \theta$  distributions from analysis set 1, both unweighted (filled circles) and weighted (open triangles), with fits to the form given in Eq. (3).

to  $R$  were good; the average  $\chi^2/\text{df}$  was 0.96. The weighted average of  $\delta$  for all 18 analysis sets is  $\delta = (-1.3 \pm 3.0) \times 10^{-4}$ , where the error is statistical, with  $\chi^2 = 24$ . The corresponding raw asymmetry is  $A_{\Xi\Lambda}(\text{raw}) = (2.2 \pm 5.1) \times 10^{-4}$ .

The background-corrected asymmetry was determined as follows. The asymmetries in the mass sidebands 1.290 – 1.310 GeV/ $c^2$  and 1.334 – 1.354 GeV/ $c^2$  were found, using weights from the central region. The weighted average of the two sideband asymmetries, scaled by the average background fraction of 0.42%, was subtracted from the raw asymmetry to give  $A_{\Xi\Lambda} = (0.0 \pm 5.1) \times 10^{-4}$ .

The analysis algorithm and its implementation were verified by a simulation, called the collimator hybrid Monte Carlo (CHMC), that used momenta and positions at the collimator exit from real  $\Xi^-$  and  $\Xi^+$  events as input to computer-generated  $\Xi$  decays. Using zero and near-zero input asymmetries, the extracted values of  $A_{\Xi\Lambda}$  differed from the input values by  $(-1.9 \pm 1.6) \times 10^{-4}$ . Note that the measurement of  $A_{\Xi\Lambda}$  has no Monte Carlo dependence.

Systematic errors were small for several reasons. First, common biases were suppressed by taking the ratio of the  $p$  and  $\bar{p} \cos \theta$  distributions. Second, overall efficiency differences do not cause a bias, only spatially dependent differences. Finally, since the polar axis changes from event to event in the lambda helicity frame, there is only a weak correlation between any particular region of the apparatus and  $\theta$ , minimizing biases due to localized differences in detector efficiencies. Table I lists the systematic errors; added in quadrature they give  $4.4 \times 10^{-4}$ .

The largest systematic error was due to the uncertainty in the calibrations of the Hall probes in the analyzing magnets. The magnetic fields were quite stable: variations in the Hall probe readings of the sum of the two fields were 6.3 G and 5.7 G (rms), respectively, for the 9024 positive and 2396 negative-polarity spills used in this analysis. From calibrations before and after the run-

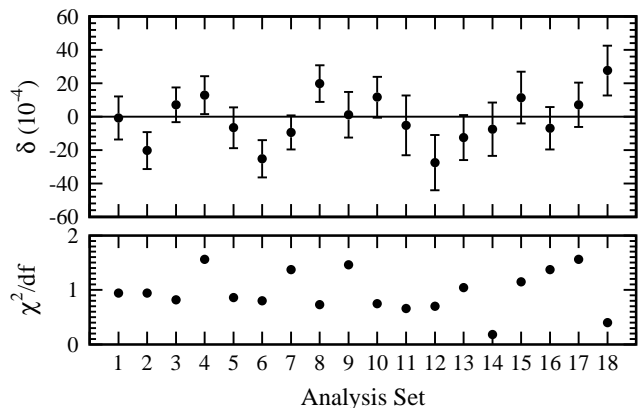


FIG. 4: Asymmetry  $\delta$  (top) and  $\chi^2/\text{df}$  (bottom) versus Analysis Set.

TABLE I: Systematic errors.

Source	Error ( $10^{-4}$ )
Analyzing magnets field uncertainties	2.4
Calorimeter inefficiency uncertainty	2.1
Validation of analysis code	1.9
Collimator exit $x$ slope cut	1.4
Collimator exit $x$ position cut	1.2
MWPC inefficiency uncertainty	1.0
Hodoscope inefficiency uncertainty	0.3
Particle/antiparticle interaction differences	0.9
Momentum bin size	0.4
Background subtraction uncertainty	0.3
Error on $\alpha_{\Xi\Lambda}$	0.03

ning periods using more precise NMR probes, the uncertainty was estimated to be 5.5 G for the sum of the fields, corresponding to an uncertainty of  $2.4 \times 10^{-4}$  in  $A_{\Xi\Lambda}$ .

The differences in efficiencies of the calorimeter, hodoscopes, and MWPCs between positive and negative running, were not corrected for, as they were negligibly small. The effect of calorimeter inefficiency differences was determined using a data sample taken with the LR trigger. The difference in  $A_{\Xi\Lambda}$ , with and without the calorimeter trigger requirement, was found to be consistent with zero, with a statistical error of  $2.1 \times 10^{-4}$ . Weighting events to correct for the hodoscope inefficiencies changed  $A_{\Xi\Lambda}$  by only  $0.3 \times 10^{-4}$ . The effect of MWPC inefficiency differences ( $1.0 \times 10^{-4}$ ) was estimated using CHMC data by determining the difference in  $A_{\Xi\Lambda}$  using real and 100% efficiencies.

The effect on  $A_{\Xi\Lambda}$  of tighter cuts on the (unweighted)  $\Xi$   $x$  slope and position at the collimator exit was studied and resulted in respective uncertainties of  $1.4 \times 10^{-4}$  and  $1.2 \times 10^{-4}$ . The effect of the bin sizes used in extracting the event weights was investigated by increasing and decreasing the  $\Xi$  momentum bin sizes by 25%,  $A_{\Xi\Lambda}$  being most sensitive to momentum. Another possible source of bias was a momentum-dependent differential loss of events due to interactions of the  $\Xi^-$  and  $\Xi^+$  decay products with material in the spectrometer. Monte Carlo studies, using the interaction cross sections given in Ref. [14], showed this bias was negligible.

The result was stable with respect to time,  $\Xi$  momentum, and secondary-beam intensity. Differences between the  $\Xi^-$  and  $\Xi^+$  production angles could in prin-

ciple cause a bias due to production polarization differences. Average production angle differences were only  $\approx 0.02$  mrad. Assuming a linear dependence of the polarization on transverse momentum [15], Monte Carlo studies indicated a negligible effect on the  $p$  and  $\bar{p} \cos \theta$  slopes. No dependence of  $A_{\Xi\Lambda}$  on production angle or incident proton beam position was evident.

To conclude, we have measured  $A_{\Xi\Lambda}$  to be  $[0.0 \pm 5.1(\text{stat}) \pm 4.4(\text{syst})] \times 10^{-4}$ . This result is consistent with standard-model predictions and is a factor of 20 improvement over the best previous result [12].

The authors are indebted to the staffs of Fermilab and the participating institutions for their vital contributions. This work was supported by the U.S. Department of Energy and the National Science Council of Taiwan, R.O.C. E.C.D. and K.S.N. were partially supported by the Institute for Nuclear and Particle Physics. K.B.L. was partially supported by the Miller Institute.

---

\* To whom correspondence should be addressed. Electronic address: craigdukes@virginia.edu.

- [1] J. Christenson *et al.*, Phys. Rev. Lett. **13**, 138 (1964); A. Alavi-Harati *et al.*, Phys. Rev. Lett. **83**, 22 (1999); V. Fanti *et al.*, Phys. Lett. B **465**, 335 (1999).
- [2] For a review, see T.E. Browder and R. Faccini, Annu. Rev. Nucl. Part. Sci. **53**, 353 (2003).
- [3] N.G. Deshpande, X.-G. He, and S. Pakvasa, Phys. Lett. B **326**, 307 (1994).
- [4] J. Tandean, Phys. Rev. D **69**, 076008 (2004).
- [5] A. Pais, Phys. Rev. Lett. **3**, 242 (1959).
- [6] T.D. Lee and C.N. Yang, Phys. Rev. **108**, 1645 (1957).
- [7] J. Tandean and G. Valencia, Phys. Rev. D **67**, 056001 (2003).
- [8] M. Huang *et al.*, Phys. Rev. Lett. **93**, 011802 (2004); A. Chakravorty *et al.*, Phys. Rev. Lett. **91**, 031601 (2003).
- [9] J.F. Donoghue and S. Pakvasa, Phys. Rev. Lett. **55**, 162 (1985); J.F. Donoghue, X.-G. He, and S. Pakvasa, Phys. Rev. D **34**, 833 (1986); D. Chang, X.-G. He, and S. Pakvasa, Phys. Rev. Lett. **74**, 3927 (1995).
- [10] X.-G. He, H. Murayama, S. Pakvasa, and G. Valencia, Phys. Rev. D **61**, 071701(R) (2000).
- [11] C.-H. Chen, Phys. Lett. B **521**, 315 (2001).
- [12] K.B. Luk *et al.*, Phys. Rev. Lett. **85**, 4860 (2000).
- [13] R.A. Burnstein *et al.*, hep-ex/0405034.
- [14] S. Eidelman *et al.* (Particle Data Group), Phys. Lett. B **592**, 1 (2004).
- [15] P.M. Ho *et al.*, Phys. Rev. D **44**, 3402 (1991).